TAMPERE UNIVERSITY OF TECHNOLOGY

Statistical analysis of BPSK-like techniques for the acquisition of Galileo signals

Elena Simona Lohan[*]

Tampere University of Technology
P.O. Box 553, FIN-33101, Tampere, Finland
elena-simona.lohan@tut.fi

The main modulation types selected for future Galileo signals are sine and cosine Binary-Offset-Carrier (SinBOC/CosBOC) modulations. On one hand, BOC-modulated signals have a narrower main lobe of their Autocorrelation Function (ACF), which allows a better accuracy in the delay tracking process. On the other hand, the acquisition process becomes more complex, due to the ambiguities in the ACF, which impose a large number of timing hypotheses for accurate detection of the signal. Several BPSK-like methods have been proposed in the literature so far and they are based on the idea that the BOC-modulated signal can be seen as a superposition of two BPSK-modulated signals, located at negative and positive subcarrier frequencies. If only one band (i.e., positive or negative) is used, we have a single SideBand (SB) technique. If both bands are used (and combined non-coherently) we have a dual SB technique. While removing the non-ambiguities in the ACF, both single and dual SB techniques suffer of performance degradation compared to a pure BPSK method, due to the non-coherent processing and to the deterioration of the correlation function properties after filtering or band selection. This paper proposes a comprehensive theoretical analysis of the properties of the BPSK-like techniques, based on the statistics of the detection variables, obtained from the simulations.

I. Background and motivation

Binary-Offset-Carrier modulation families[1] are the main proposals for the modulation type of Galileo Open Services (OS) and Publicly Regulated Services (PRS) signals. Their main advantage is a better use of the spectrum, which makes the separation with GPS signals easier,[1].[2] Compared with the classical BPSK-modulated pseudorandom (PRN) code, a BOC-modulated PRN signal has additional peaks in the autocorrelation function. The width of the main lobe of the ACF decreases (compared with BPSK, where the main lobe width is 2 chips), but additional sidelobes appear in the 2-chip interval, which makes the ACF to become "ambiguous",[3].[4] This translates to the fact that the step $(\Delta t)_{bin}$ of searching the time bins in the acquisition process should be sufficiently small, in order to be able to detect the main lobe of the ACF (i.e., we need a higher number of timing hypotheses in order to search a given time-uncertainty window compared to BPSK case).[5] Thus, the acquisition becomes more computationally expensive, the computational load being inversely proportional with the time-bin size (or step) $(\Delta t)_{bin}$.[5] This step should be, typically, about half of the width of the main lobe, which, in its turn, is dependent on the modulation order N_{BOC} (defined here as twice the ratio between the sub-carrier frequency f_{sc} and the chip rate f_c, according to[6]). For example, for SinBOC(1,1) case, proposed for Galileo OS,[7] we have $2N_{BOC} - 1 = 3$ significant lobes of the absolute value of the ACF and the width of the main lobe of the ACF envelope can be easily computed as 0.68 chips.

---

[*]Senior Researcher within the Institute of Communications Engineering.

In order to avoid the ambiguities of the ACF and to be able to increase the step between timing hypotheses in the acquisition process (and thus, to decrease the acquisition time), the so-called 'BPSK-like' techniques have been proposed in the literature,[3],[4],[5].[8] The 'BPSK-like' techniques remove the effect of the sub-carrier modulation, by implementing a pair of single sideband correlation receivers, which might be used individually (single SB case) or combined non-coherently (dual SB case).

The main disadvantage of the BPSK-like techniques is the presence of some correlation losses (compared with a BPSK-modulated signal), mentioned in,[3],[4],[5] but not analyzed theoretically so far. The goal of our paper is to introduce a theoretical analysis of the BPSK-like techniques for the derivation of the expected detection probability and Mean Acquisition Times (MAT). The theoretical analysis is based on chi-square central and non-central distributions of the decision variables and the parameters of these distributions are estimated based on simulation results. We will show that the variances and non-centrality parameters for these distributions are distinct for SinBOC and CosBOC cases, and they are dependent on the modulation order for SinBOC cases. These results had not been shown before, to the author's knowledge.

Three cases will be discussed here: the ambiguous-BOC approach, the non-ambiguous single-SB technique and the non-ambiguous dual-SB technique. The BPSK case is also kept as a performance bound, in order to illustrate the gap between the 'BPSK-like' techniques and the true BPSK case. We present a comprehensive approach for computing the detection probability for the serial search, by taking into account all the possible timing hypotheses (this is different from,[4] where only one timing hypothesis is considered at a time). We also discuss the impact of small frequency errors on the performance on each algorithm. The detection probability curves are presented for CosBOC(15,2.5)-modulated pseudorandom codes with the parameters taken from Galileo proposals for PRS signals, which have an increased number of ambiguities, and therefore, are likely to benefit the most from 'BPSK-like' approaches.

II.   BPSK-like techniques

The block diagrams of the **single-SB method** is illustrated in Fig. 1, for Upper SideBand (USB) processing,[5].[8] The same is valid for the Lower SideBand (LSB) processing. The main lobe of one of the sidebands
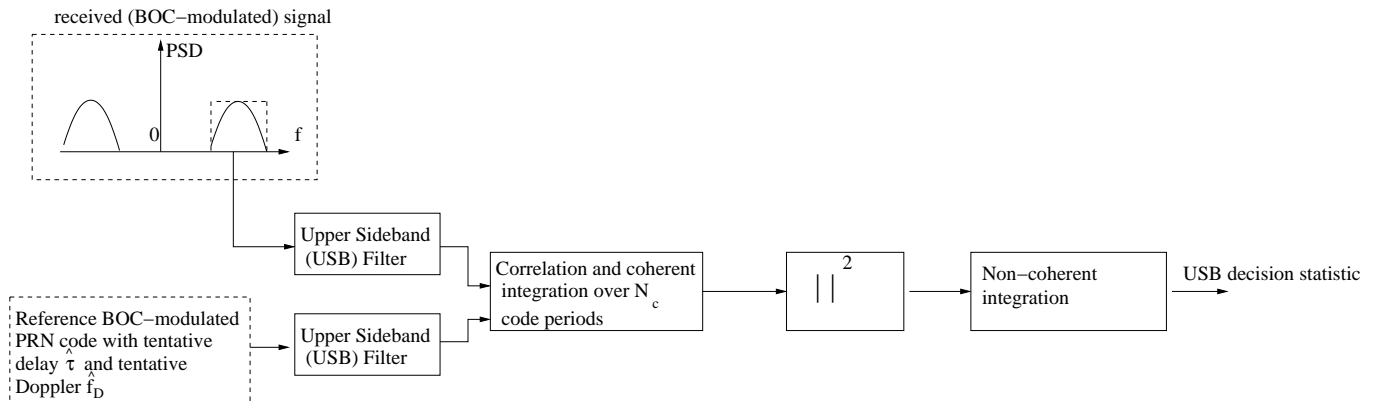

Fig. 1   Block diagram of single sideband processing (here, upper sideband).

of the received signal (upper or lower) is selected via filtering and correlated with a reference code, with tentative delay $\widehat{\tau}$ and reference Doppler frequency $\widehat{f_D}$. The reference code is obtained in a similar manner with the received signal, hence the autocorrelation function is no longer the ACF of a BOC-modulated signal, but it will resemble the ACF of a BPSK-modulated signal. However, the exact shape of the resulting ACF is not identical with the ACF of a BPSK-modulated signal, since some information is lost when filtering out the sidelobes adjacent to the main lobe. This filtering is needed in order to reduce the noise power.

When the **dual-SB method** is used, we add together the USB and LSB outputs and form the dual SB statistic. The 'BPSK-like' techniques refer to single and dual SB processing.

The **ambiguous-BOC processing** means that the received signal is directly correlated with the reference BOC-modulated PRN sequence (all the spectrum is used for both the received signal and reference code). The **BPSK case** refers to the situation when the transmitted signal is BPSK modulated and the correlation is done with a reference BPSK-modulated PRN code.
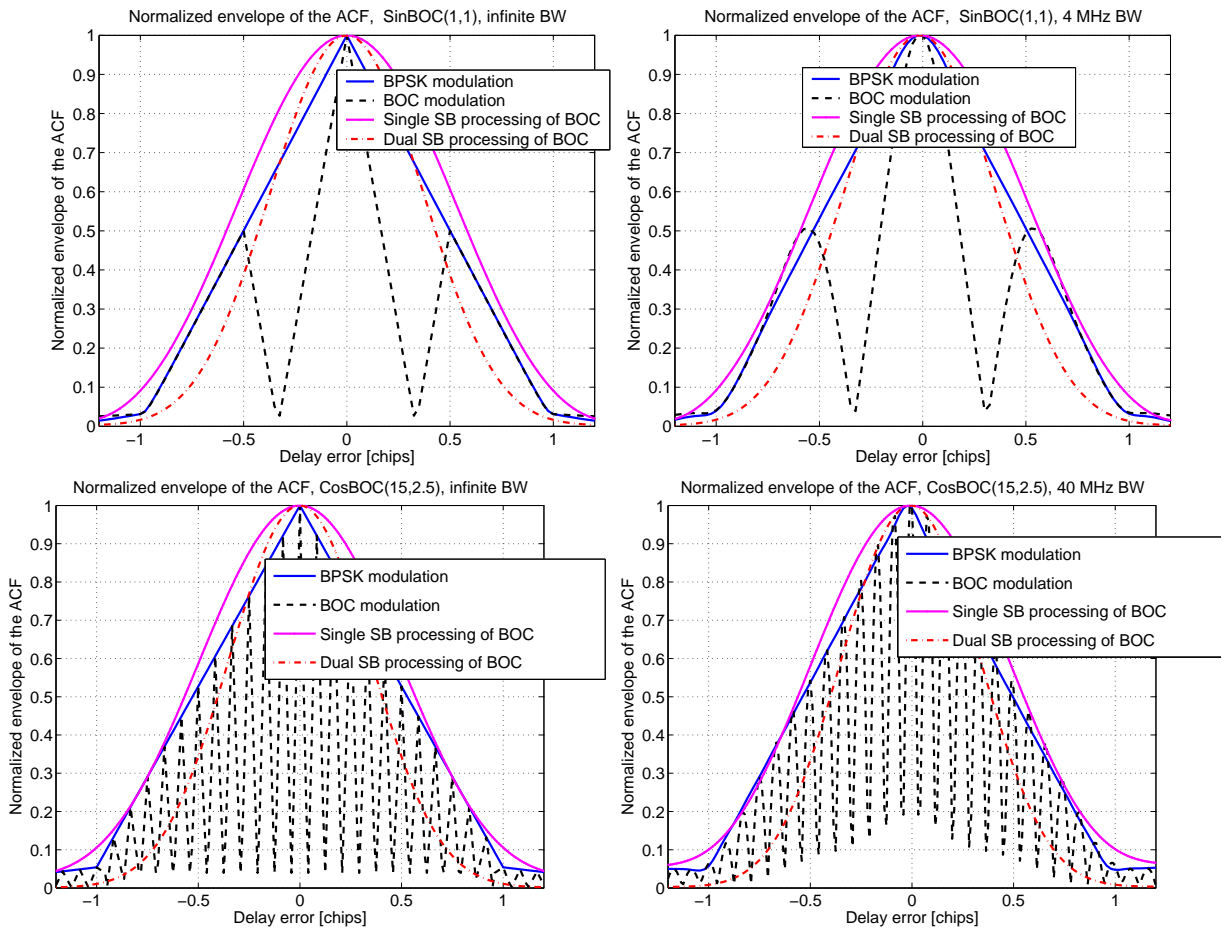

Fig. 2 Shape of the envelope of the autocorrelation function for BPSK, BOC and BPSK-like waveforms with different front-end bandwidths. OS signals (upper plots) and PRS signals (lower plots).

Examples of the ACF shape after single and dual SB processing are shown in Fig. 2, for SinBOC(1,1) and, respectively, CosBOC(15,2.5) signals, currently selected for OS and PRS services.[9] The ambiguous-BOC waveform and the reference-BPSK case are also shown. In the left plots, the signal before SB processing is assumed to have infinite bandwidth (BW), hence, we have sharp peaks in the BOC waveform. The filters for SB processing are assumed to be ideal rectangular filters. The effect of non-ideal filtering on the ACF waveforms is shown in the right plots of Fig. 2. Here, Finite Impulse Response (FIR) filters of bandwidths 4 MHz and 40 MHz have been used for OS and PRS, respectively. We notice that the peaks of the ACF become flatter, and the fades of the ACF may have a fluctuating level (e.g., lower right plot of Fig. 2). Non-constant group delay filters (such as Chebyshev or Butterworth) may introduce some additional, non-constant, delay in the ACF, which should be taken into account during the synchronization process, as emphasized in.[4] In what follows, we will focus on the infinite bandwidth situation, since this case will give the bound on the performance of the discussed techniques.

III. Statistical modelling of decision variables

The decision statistic $Z_{method}(\Delta\widehat{\tau}, \Delta\widehat{f_D})$ is the output of the non-coherent integration, depending on the delay error $\Delta\widehat{\tau}$ and Doppler error $\Delta\widehat{f_D}$. Here, the method refers to one of the following cases, discussed in the previous Section: ambiguous BOC (BOC), single SB (SSB), dual SB (DSB), or $BPSK$ (i.e., BPSK modulation was used at the transmitter).

We assume that coherent integration is done over N_c code epochs (one code epoch has a duration $S_F T_c$, where S_F is the spreading factor of the PRN code and $T_c = 1/f_c$ is the chip interval), followed by non-coherent integration on N_{nc} blocks. Obviously, if the delay error is higher (in absolute value) than one chip (i.e., $|\Delta\widehat{\tau}| \geq T_c$) or the Doppler error is higher than the inverse of the coherent integration time (i.e., $|\Delta\widehat{f_D}| \geq 1/(N_c S_F T_c)$), we are in an incorrect bin, i.e., the test statistic is based on noise only. If $|\Delta\widehat{\tau}| \geq T_c$ and $|\Delta\widehat{f_D}| \geq 1/(N_c S_F T_c)$, we are in a correct bin, i.e., the test statistic includes both signal and noise. Depending on the step of searching the time and frequency bins, we may have several correct bins. In what follows, we assume that the step between the frequency hypotheses is the inverse of the coherent integration time $1/(N_c S_F T_c)$ and the step between timing hypotheses is $(\Delta t)_{bin}$ (less than one chip). Therefore, we may have $N_t = \lfloor \frac{2T_c}{(\Delta t)_{bin}} \rfloor$ correct timing hypotheses, where $\lfloor x \rfloor$ stands for the highest integer smaller or equal to x.

For BOC and $BPSK$ cases, it is well known that the distribution of $Z_{BOC}(\cdot)$ and $Z_{BPSK}(\cdot)$ is a central or non-central chi-square distribution, according to whether we are in an incorrect or a correct bin, respectively,[4],[10],[11].[12] This is valid in static channels and it is due to the fact that the output of the coherent integration is a complex Gaussian variable, due to the additive white noise real and imaginary parts. The underlying chi-square distributions have $2N_{nc}$ degrees of freedom and a variance equal to $\sigma_{nb}^2/(N_c N_{nc})$, where σ_{nb}^2 is the narrowband noise spectral power density (double-sided), related to the Carrier-to-Noise Ratio (CNR) as follows:[12]

$$\sigma_{nb}^2 = E_b 10^{-\frac{CNR[dB/Hz]-30}{10}} \tag{1}$$

Above, E_b is the signal energy (per transmitted code epoch, which is equal here to $S_F T_c = 1$ ms). The square-root λ of the non-centrality parameter of the non-central chi-square distribution is a function $\mathcal{F}(\cdot)$ of the delay and Doppler errors as follows,[4]:[12]

$$\lambda = \sqrt{E_b}\mathcal{F}(\Delta\widehat{\tau}, \Delta\widehat{f_D}) = \sqrt{E_b}\left|\mathcal{R}(\Delta\widehat{\tau})\frac{sin(\pi\Delta\widehat{f_D}T_{coh})}{\pi\Delta\widehat{f_D}T_{coh}}\right|, \tag{2}$$

where $\mathcal{R}(\Delta\widehat{\tau})$ is the ACF value at delay error $\Delta\widehat{\tau}$ for the BOC-modulated PRN code, and $T_{coh} = N_c S_F T_c$ is the coherent integration time.

When single or dual SB methods are used, the test statistics $Z_{SSB}(\cdot)$ and $Z_{DSB}(\cdot)$ are expected to be also chi-square distributed (central or non-central), due to the fact that, applying a linear filter on a complex Gaussian distribution preserves the same distribution at the output. However, the variance and non-centrality parameter are likely to be changed, due to the fact that only the main lobe of the signal spectrum is used at the receiver.

In order to find the exact values for the variance and non-centrality parameter for single and dual SB, we carried out several simulations for various SinBOC and CosBOC modulations and for various delay and Doppler errors. The resulting parameters are summarized in Table 1 and eq. (3), and some examples of the distribution matching between theory and simulations are shown in Fig. 3. The simulations were carried out for an oversampling factor of $N_s = 2$ sub-samples per BOC interval.

In Table 1, x is a parameter accounting for the correlation losses and filtering effects in the single and dual SB processing. Simulation results showed that the best distribution matches are obtained for x slightly higher than the energy per main lobe, as follows:

$$x = \begin{cases} 0.5 & \text{for SinBOC with } N_{BOC} = 2 \\ 0.39 & \text{for CosBOC } \forall\ N_{BOC} \end{cases} \tag{3}$$

Table 1 Parameters of the central and non-central chi-square distributions of the test statistic $Z_{method}(\cdot)$.

Method	Variance σ^2	Square-root of non-centrality parameter λ (if correct bin)	Degrees of freedom N_{deg}
BOC/BPSK	$\sigma_{nb}^2/(N_c N_{nc})$	$\sqrt{E_b}\mathcal{F}(\Delta\widehat{\tau}, \Delta\widehat{f_D})$	$2N_{nc}$
Single SB	$x\sigma_{nb}^2(N_c N_{nc})$	$x\sqrt{E_b}\mathcal{F}(\Delta\widehat{\tau}, \Delta\widehat{f_D})$	$2N_{nc}$
Dual SB	$x\sigma_{nb}^2/(N_c N_{nc})$	$x\sqrt{2E_b}\mathcal{F}(\Delta\widehat{\tau}, \Delta\widehat{f_D})$	$4N_{nc}$

Intuitively, the values given by eq. (3) for the parameter x can be explained due to some correlation losses associated with the filtering and due to the modification of the reference code (which can be seen as a decrease of the non-centrality parameter), together with some decrease in the noise variance (due to the filtering of the signal and noise, as seen in Fig. 1). The x parameter should be (intuitively) close to the fraction of power per main lobe of the power spectral density of the BOC-modulated signal, an assumption which is indeed verified by our results (e.g., the power per main lobe of the SinBOC(1,1) signal is around 0.4279 of the total power, if the total power was normalized to 1, and the value for x, namely $x = 0.5$ for SinBOC(1,1), is slightly above this fraction).

For SinBOC modulation of higher orders, different values of x have been found, such as $x = 0.46$ for $N_{BOC} = 3, 4, 5, 6$ and $x = 0.41$ for $N_{BOC} = 7$. Typically, the higher N_{BOC} order, the higher are the correlation losses. On the other hand, due to an increased number of fades in the envelope of the ACF of a sine or cosine-BOC modulation with high N_{BOC}, the benefit of using a BPSK-like method for high modulation orders could be quite significant in terms on CNR as the simulation results will show.

The number of degrees of freedom for dual SB method (see Table 1) is $4N_{nc}$, because, before the non-coherent integration process, we have 4 real Gaussian variables, coming from the real and imaginary parts of the noise in the upper band, and respectively in the lower band.[10]

Examples of the simulation-based normalized histogram and the theoretical chi-square Probability Distribution Function (PDF) for correct and incorrect bins are shown in Fig. 3, for SinBOC(1,1) and Cos-BOC(15,2.5), respectively. The considered correct bin has $\Delta\widehat{\tau} = 0$ and a small Doppler error, specified in the figure caption. We remark that similar good matching has been obtained for various other CNR levels, Doppler errors, coherent and non-coherent integration times and BOC modulation orders.

The Cumulative Distribution Function (CDF) under correct and incorrect-bin hypotheses can be written as[13]

$$
\begin{cases}
F_c(z) = 1 - \displaystyle\sum_{k=0}^{N_{deg}/2-1} e^{-\frac{z}{\sigma^2}} \left(\frac{z}{\sigma^2}\right)^k \frac{1}{k!} & \text{in incorrect bins} \\[4mm]
F_{nc}(z, \lambda) = 1 - Q_{N_{deg}/2}\left(\frac{\lambda\sqrt{2}}{\sigma}, \frac{\sqrt{2z}}{\sigma}\right) & \text{in correct bins,}
\end{cases}
\tag{4}
$$

with σ^2, N_{deg}, and λ given in Table 1 and $Q_{N_{deg}/2}(\cdot)$ being the generalized Marcum-Q function.[13]

IV. Detection-probability and MAT computation for serial search acquisition

The detection probability per bin $P_{d_{bin}}(\Delta\widehat{\tau})$ is the probability that the decision variable is higher than a decision threshold γ, provided that we are in a correct bin (hypothesis $\mathcal{H}_1$). Similarly, the false alarm probability P_{fa} is the probability that the decision variable is higher than γ, provided that we are in an incorrect bin (hypothesis $\mathcal{H}_0$. From the definition of the CDF, it follows that

$$
\begin{cases}
P_{d_{bin}}(\Delta\widehat{\tau}, \Delta\widehat{f_D}) &= 1 - F_{nc}(\gamma, \lambda) \\
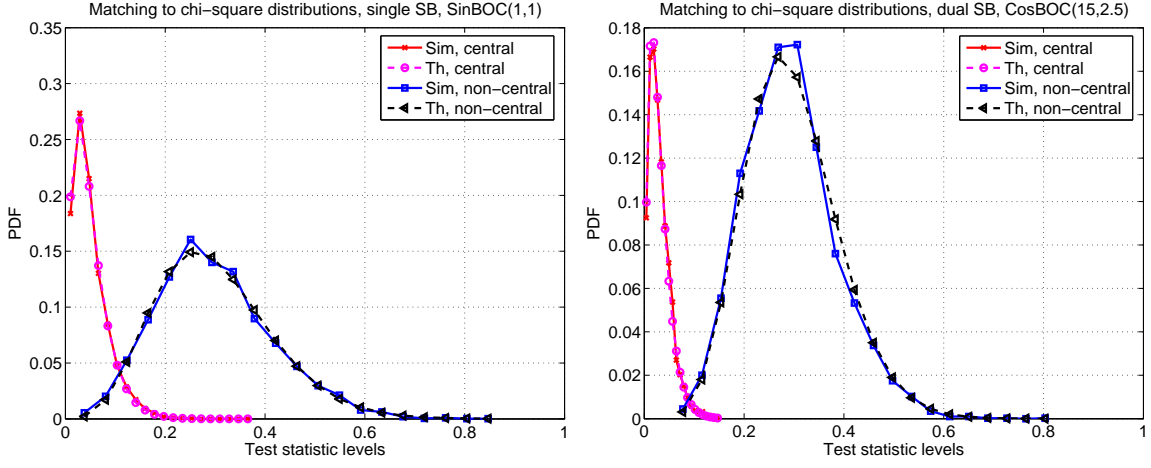P_{fa} &= 1 - F_c(\gamma)
\end{cases}
\tag{5}
$$

Fig. 3   Matching between theoretical (Th) and simulation-based (Sim) distributions of the test statistic $Z_{method}(\cdot)$ **for single and dual SB. Upper: SinBOC(1,1), single SB, CNR=30 dB/Hz,** $N_c = 10$, $N_c = 2$, $\Delta\widehat{f_D} = 0$ **Hz. Lower: CosBOC(15,2.5), dual SB, CNR=35 dB/Hz,** $N_c = 8$, $N_c = 1$, $\Delta\widehat{f_D} = 25$ **Hz.**

Above, λ (and, thus, $P_{d_{bin}}$ also) is dependent on the method and on the delay and Doppler errors associated with the considered bin. Since we have several (i.e., N_t) correct bins, the global detection probability P_d can be computed as follows:

$$P_d(\Delta\tau_0) = \sum_{k=0}^{N_t-1} P_{d_{bin}}\big(\Delta\tau_0 + k(\Delta t)_{bin}, \Delta\widehat{f_D}\big)$$
$$\times \prod_{i=0}^{k-1}\Big(1 - P_{d_{bin}}(\Delta\tau_0 + i(\Delta t)_{bin}, \Delta\widehat{f_D})\Big) \tag{6}$$

that is, the sum of probabilities of detecting the signal in the i-th bin, provided that all the previous tested hypotheses for the prior correct bins gave a mis-detection. In eq. (6), $\Delta\tau_0$ is the delay error associated with the first sampling point in the two-chip interval where we have the N_t correct bins. Eq. (6) is valid only for fixed sampling points. However, due to the random nature of the channels, the sampling point (with respect to the channel delay) is randomly fluctuating, hence, the global P_d will be computed as the expectation operator $\mathbf{E}(\cdot)$ over all possible initial delay errors (under uniform distribution, we simply take the temporal mean):

$$P_d = \mathbf{E}_{\Delta\tau_0}\big(P_d(\Delta\tau_0)\big). \tag{7}$$

Fig. 4 illustrates the idea of computing the global P_d. Here, two possible sampling sequences are shown. The total number of sampling sequences depends on a discrete step, chosen sufficiently small. The step of searching the time bins in this figure is $(\Delta t)_{bin} = 0.2$ chips.

The mean acquisition time $\overline{T}_{acq}$ for the serial search can be computed according to the global P_d, the false alarm P_{fa}, the penalty time $K_{penalty}$ and the total number of bins in the search space q:[4]

$$\overline{T}_{acq} = \frac{2 + (2 - P_d)(q - 1)(1 + K_{penalty}P_{fa})}{2P_d}\tau_d, \tag{8}$$

where $\tau_d = N_c N_{nc} S_F T_c$ is the dwell time, and P_d and P_{fa} are given by eqs. (5) to (8).
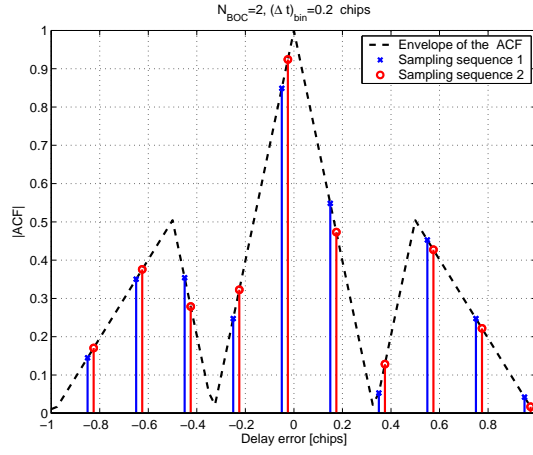
Fig. 4 Examples of sampling sequences capturing the N_t possible correct bins for the decision statistic of a SinBOC(1,1)-modulated signal; ambiguous BOC method.

V.   Simulation results

In the simulations, we considered PRN codes of length $S_F = 1023$, modulated via CosBOC$(15, 2.5)$ modulation (i.e., PRS signals). The false alarm probability was assumed to be $P_{fa} = 10^{-3}$. The detection threshold γ was computed according to this P_{fa}, and used then in the calculus of P_d. The MAT curves may be easily derived from eq. (8) and from the detection probability curves.

The detection probability for various CNR values, assuming a step of $\Delta\widehat{\tau} = 0.05$ chips or 0.5 chips, respectively, is shown in Fig. 5. As seen in Fig. 5, there is a significant gain in terms of detection probability if we use a BPSK-like technique and a step of 0.5 chips, instead of using the ambiguous-BOC method. On the other hand, if the step is small (less than half of the main lobe of the ACF), there is only slight improvement of a single-SB technique versus the ambiguous-BOC case, and only about 1 dB gain of the dual-SB technique versus the ambiguous-BOC case. Due to the processing losses, BPSK-like techniques
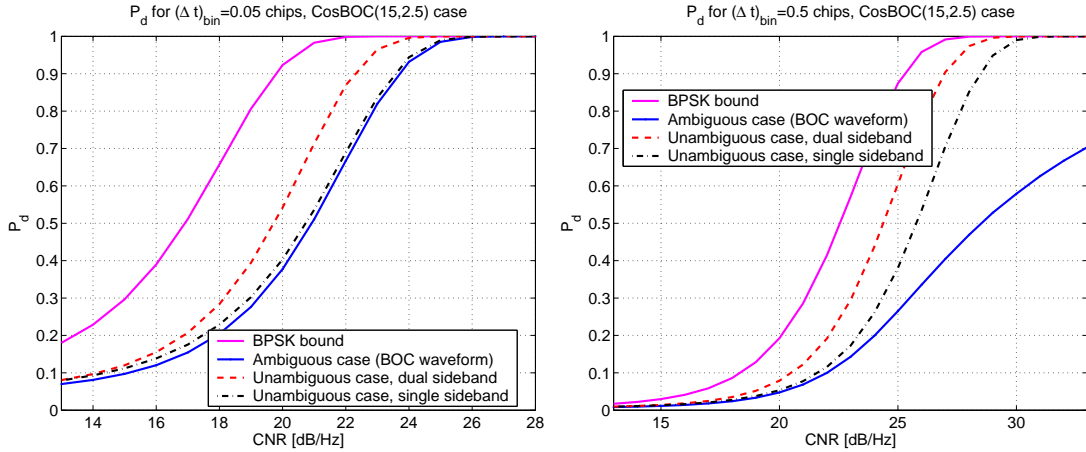

Fig. 5 Detection probability as functions of CNR for CosBOC(15,2.5) and two steps $\Delta\widehat{\tau} = 0.05$ chips (upper) and $\Delta\widehat{\tau} = 0.5$ chips (lower). $\Delta\widehat{f_D} = 0$, $N_c = 40$ ms; $N_{nc} = 1$ blocks.

are quite far from the BPSK bound, but they still offer improvement over the ambiguous-BOC processing.

The impact of frequency errors on the P_d is shown in Fig. 6 for $N_c = 40$ ms. All the considered methods suffer of fast performance deterioration when the Doppler errors increases above one fifth of the coherent
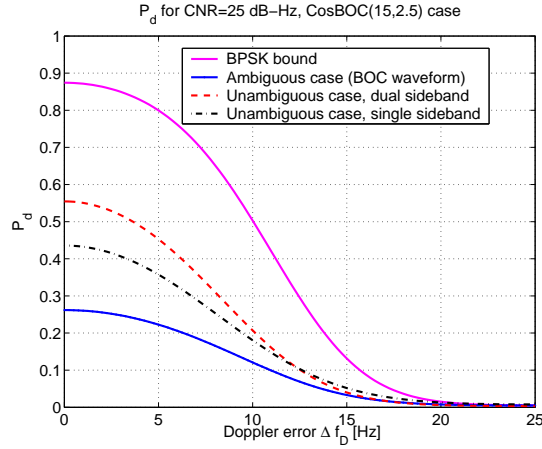
integration time.

Fig. 6 Detection probability as functions of the small Doppler error $\Delta \widehat{f_D}$, CosBOC(15,2.5), CNR=25 dB/Hz; $N_c = 40$ ms; $N_{nc} = 1$ blocks, $\Delta \widehat{\tau} = 0.5$ chips.

We also remark from Fig. 5, that the losses reported in[5] (of 3 dB of single-SB compared to BPSK bound and of 0.5 dB of dual-SB compared with BPSK bound) are not always true, and they depend on the step $((\Delta t)_{bin})$ and on the modulation order. For example, for a step $(\Delta t)_{bin} = 0.5$ chips, the losses are higher than given in[5] for dual SB of CosBOC(15,2.5) modulation (we loose about 1.5 dB when using dual-SB processing compared to BPSK bound).

VI.   Conclusions

In this paper, we presented a theoretical analysis of the BPSK-like methods in the context of BOC-modulated signals for serial search acquisition. Our analysis was based on the statistical modelling of the decision variables in the acquisition process. We also presented a comprehensive approach for computing the detection probability for the serial search, by taking into account all the possible timing hypotheses. We showed that there is significant gain in terms of detection probability if dual-SB technique is used to remove the ambiguities of the correlation function, since higher steps of searching the timing hypotheses can be employed. We also showed that both BPSK-like techniques (single and dual SB) do not reach the BPSK bound. We also illustrated the effect of small residual Doppler frequency errors on the performance of BPSK-like algorithms.

Acknowledgments

VII.   References

[1]J. Betz, "The Offset Carrier Modulation for GPS modernization," in *Proc. of ION Technical meeting*, pp. 639–648, 1999.

[2]J. Betz and D. Goldstein, "Candidate Designs for an Additional Civil Signal in GPS Spectral Bands." MITRE Technical Papers, Jan 2002.

[3]N. Martin, V. Leblond, G. Guillotel, and V. Heiries, "BOC(x,y) signal acquisition techniques and performances," in *Proc. of ION-GPS2003*, (Portland, OR, US), pp. 188–198, Sep 2003.

[4]V. Heiries, D. Oviras, L. Ries, and V. Calmettes, "Analysis of non ambiguous BOC signal acquisition performance," in *CDROM Proc. of ION GNSS*, (Long Beach, CA), Sep 2004.

[5]P. Fishman and J. Betz, "Predicting performance of direct acquisition for the M-code signal," in *Proc. of ION NMT*, pp. 574–582, 2000.

[6] E. Lohan, A. Lakhzouri, and M. Renfors, "A novel family of Binary-Offset-Carrier modulation techniques with applications in satellite navigation systems." Submitted to Wiley International Journal of Wireless Communications and Mobile Computing, 2004.

[7] J. Betz and B. Titus, "Intersystem and intrasystem interference with signal imperfections." MITRE Technical Papers, Jan 2004.

[8] J. Betz and P. Capozza, "System for direct acquisition of received signals." US Patent Application Publication 2004/0071200 A1, Apr 2004.

[9] G. Hein, M. Irsigler, J. A. Rodriguez, and T. Pany, "Performance of Galileo L1 signal candidates," in *CDROM Proc. of European Navigation Conference GNSS*, May 2004.

[10] S. Fischer, A. Guerin, and S. Berberich, "Acquisition concepts for Galileo BOC(2,2) signals in consideration of hardware limitations," in *Proc. of IEEE Vehicular Technology Conference*, vol. 5, pp. 2852–2856, May 2004.

[11] A. Schmid and A. Neubauer, "Theoretical minimal bounds for single shot measurement thresholds of the Galileo and GPS open signals in multipath fading environments," in *CDROM Proc. of European Navigation Conference ENC-GNSS*, 2004.

[12] F. Bastide, O. Julien, C. Macabiau, and B. Roturier, "Analysis of L5/E5 acquisition, tracking and data demodulation thresholds," in *Proc. of ION-GPS*, pp. 2196–2207, 2002.

[13] J. Proakis, *Digital communications*. New York: McGRAW-Hill Int. Edition, 4th ed., 2001.